Structural Engineering and Mechanics, Vol. 6, No. 6 (1998) 711-725
DOI: http://dx.doi.org/10.12989/sem.1998.6.6.711

Stabilization of pressure solutions in four-node quadrilateral elements

Sang-Ho Lee† and Sang-Hyo Kim‡

Department of Civil Engineering, Yonsei University, Seoul 120-749, Korea

Abstract. Mixed finite element formulations for incompressible materials show *pressure oscillations* or *pressure modes* in four-node quadrilateral elements. The criterion for the stability in the pressure solution is the so-called Babuška-Brezzi stability condition, and the four-node elements based on mixed variational principles do not appear to satisfy this condition. In this study, a pressure continuity residual based on the pressure discontinuity at element edges proposed by Hughes and Franca is used to study the stabilization of pressure solutions in bilinear displacement-constant pressure four-node quadrilateral elements. Also, a solid mechanics problem is presented by which the stability of mixed elements can be studied. It is shown that the pressure solutions, although stable, are shown to exhibit sensitivity to the stabilization parameters.

Key words: stabilization of pressure; pressure oscillations; pressure modes; incompressible materials; mixed finite elements; volumetric locking.

1. Introduction

The four-node quadrilateral element is the workhorse of nonlinear finite element analysis because of its simplicity and versatility. However, when the element is implemented with full quadrature, it locks for incompressible materials in a phenomenon called *volumetric locking*. It is also quite stiff in bending, i.e., the displacements are underpredicted unless several layers of elements are used through the thickness.

One of the first remedies for this difficulty of volumetric locking is selective-reduced integration, Hughes (1977); Doherty *et al.* (1969) earlier used selective-reduced integration for reducing flexural stiffness. When this procedure is applied to volumetric locking, the hydrostatic, or pressure terms are integrated using a single quadrature point, whereas the deviatoric terms are evaluated by full quadrature, i.e., 2×2 Gauss quadrature. It became clear subsequently through the discovery of the equivalence principle by Malkus and Hughes (1978), that this corresponds to a formulation of the element by a multi-field principle with a constant pressure field.

In the past decade, the performance of the quadrilateral element has been enhanced by using two field (Hellinger-Reissner) and three field (Hu-Washizu) variational principles; cf. Pian and Sumihara (1984), Belytschko and Bachrach (1986) and Simo and Rifai (1990); see MacNeal (1993) for an extensive account of the mechanics of overcoming volumetric locking.

† Assistant Professor
‡ Associate Professor

Though not widely recognized, a shared property of all these elements is that for an incompressible material, the volumetric strain vanishes when the nodal displacements are such that the total volume of the element is unchanged. As a consequence, when the displacement of the nodes is such that the volume of the element is preserved, the strain field is equivoluminal throughout the element, see Belytschko and Bindeman (1991). This is the key to avoiding volumetric locking, for if the strain field is not isochoric (volume-preserving) at all quadrature points of the element, very large pressures result and "lock" the element.

Unfortunately, a byproduct of designing this property into the strain field is that the element then fails to meet the Babuška-Brezzi conditions; see Babuška (1971) and Brezzi (1974); Xue, Karlovitz and Atluri (1985) have given a form of this principle for mixed elements. As a consequence, in some meshes, the pressures alternate in sign in a phenomenon called *ckeckerboarding*, wherein the pressures alternate, see Sani *et al.* (1981) or Hughes (1987). This malady is a result of the rank-deficiency of the equations for the pressure, an excellent explanation is given in Lee, Gresho and Sani (1979). The consequence of this phenomenon is that whenever a four-node quadrilateral element is designed to avoid locking, its predictions of pressures become deficient; this is an impasse that is quite bewildering.

Hughes and Franca (1987) have developed a new methodology whereby the pressure oscillations are eliminated by adding the squares of the equilibrium equations and pressure discontinuities to the variational principle. The formulation circumvents the Babuška-Brezzi condition and makes it possible to use a natural combination of displacement and pressure interpolants. However, in the use of this formulation, the relationship between the accuracy of displacement and pressure solutions and the stability parameter needs detailed study. Silvester and Kechkar (1990) have also studied the implementation of this stabilization. Other developments for the stabilization of pressures are given by Oden *et al.* (1982), Pitkäranta and Stenberg (1984), Pitkäranta and Saarinen (1985).

In this paper, the Hughes-Franca stabilization procedure will be studied in the four-node element QBI, Belytschko and Bachrach (1986), and other mixed elements. The QBI element formulation for incompressible materials is derived from the Hu-Washizu variational principle. The accuracy of the displacement and pressure solutions are compared with those of Simo-Rifai (1990) and other mixed elements. The sensitivity of the pressure solutions to the stabilization parameters is also discussed.

2. Incompressible elasticity formulation for the stabilization of pressure

Let Ω be an open bounded region in $\boldsymbol{R}^{n_{sd}}$, where n_{sd} is the number of space dimensions ($n_{sd}=2$ or 3), with piecewise smooth boundary Γ. The standard displacement-pressure formulation of isotropic incompressible elasticity is:

$$\text{div } \boldsymbol{\sigma} + \boldsymbol{b} = 0 \qquad \text{in } \Omega, \tag{1}$$

$$\text{div } \boldsymbol{u} = 0 \qquad \text{in } \Omega, \tag{2}$$

$$\boldsymbol{\sigma} = 2\mu\boldsymbol{\varepsilon} - p\boldsymbol{I} \qquad \text{in } \Omega, \tag{3}$$

$$\boldsymbol{u} = \boldsymbol{u}^* \qquad \text{on } \Gamma_u, \tag{4}$$

$$\boldsymbol{\sigma}\cdot\boldsymbol{n} = \boldsymbol{t}^* \qquad \text{on } \Gamma_t. \tag{5}$$

Here $\boldsymbol{\sigma}$ is the Cauchy stress tensor, $\boldsymbol{b}$ is body force, $\boldsymbol{u}$ is displacement (or velocity in fluid

mechanics), μ is shear modulus (or viscosity in fluid mechanics), p is pressure, $\boldsymbol{I}$ is the identity tensor, and $\boldsymbol{\varepsilon}$ is the symmetric part of the displacement gradient. Eq. (2) gives the incompressibility condition. The boundary Γ consists of two subregions, Γ_u and Γ_t, which are the prescribed displacement and traction boundaries, respectively, and

$$\Gamma = \Gamma_u \cup \Gamma_t, \tag{6}$$

$$\phi = \Gamma_u \cap \Gamma_t. \tag{7}$$

The unit outward normal vector to Γ is denoted by $\boldsymbol{n}$.

Let $\mathcal{U}$ and $\mathcal{V}$ be the spaces of displacement trial and test functions, and $\mathcal{P}$ be the space of pressures. Let $\boldsymbol{u}$ and $\delta\boldsymbol{u}$ denote displacement trial solutions and test functions, and p and δp denote pressure trial solutions and test functions, respectively. The weak form for incompressible materials is

$$\int_\Omega \delta\boldsymbol{\varepsilon}^T \boldsymbol{\sigma}\, d\Omega - \int_\Omega \delta p\, (\operatorname{div} \boldsymbol{u})\, d\Omega = \int_\Omega \delta\boldsymbol{u}^T \boldsymbol{b}\; d\Omega + \int_{\Gamma_t} \delta\boldsymbol{u}^T \boldsymbol{t}^*\; d\Gamma \tag{8}$$

Eq. (8) can be rewritten for isotropic materials as follows by using Eq. (3)

$$\int_\Omega \delta\boldsymbol{\varepsilon}^T 2\mu\boldsymbol{\varepsilon}\, d\Omega - \int_\Omega \delta(\operatorname{div} \boldsymbol{u})^T p\; d\Omega - \int_\Omega \delta p\, (\operatorname{div} \boldsymbol{u})\, d\Omega = \int_\Omega \delta\boldsymbol{u}^T \boldsymbol{b}\; d\Omega + \int_{\Gamma_t} \delta\boldsymbol{u}^T \boldsymbol{t}^*\; d\Gamma \tag{9}$$

where the trial solutions $\boldsymbol{u}$ and p, and the test functions $\delta\boldsymbol{u}$ and δp are defined as follows:

$$\boldsymbol{u} \in \mathcal{U};\ \mathcal{U} = \{\boldsymbol{u} \mid \boldsymbol{u} \in C^o,\ \boldsymbol{u} = \boldsymbol{u}^* \text{ on } \Gamma_u\}, \tag{10}$$

$$\delta\boldsymbol{u} \in \mathcal{V};\ \mathcal{V} = \{\delta\boldsymbol{u} \mid \delta\boldsymbol{u} \in C^o,\ \delta\boldsymbol{u} = 0 \text{ on } \Gamma_u\}, \tag{11}$$

$$p \in \mathcal{P},\ \delta p \in \mathcal{P};\ \mathcal{P} = \{p \mid p \in C^{-1}\}. \tag{12}$$

The above weak formulation is not stable for pressure solutions unless specific displacement and pressure interpolations are chosen, see chapter 4 of Hughes (1987). In particular, *pressure oscillations*, or *pressure modes* (often called checkerboarding, which are caused by singularities in the global equations) occur in the bilinear displacement-constant pressure four-node quadrilateral element (Q1P0).

Hughes and Franca (1987) modified the weak formulation Eq. (9) as follows to stabilize the pressure

$$\begin{aligned}
&\int_\Omega \delta\boldsymbol{\varepsilon}^T 2\mu\boldsymbol{\varepsilon}\, d\Omega - \int_\Omega \delta(\operatorname{div} \boldsymbol{u})^T p\; d\Omega - \int_\Omega \delta p\, (\operatorname{div} \boldsymbol{u})\, d\Omega \\
&- \int_{\tilde{\Omega}} \frac{\alpha h^2}{2\mu} \delta(\operatorname{div} \boldsymbol{\sigma})^T\, (\operatorname{div}\boldsymbol{\sigma})\, d\Omega - \int_{\tilde{\Gamma}} \frac{\beta h}{2\mu} [[\delta p]]\, [[p]]\, d\Gamma \\
&= \int_{\tilde{\Omega}} (\delta\boldsymbol{u}^T + \frac{\alpha h^2}{2\mu} \delta(\operatorname{div} \boldsymbol{\sigma})^T)\boldsymbol{b}\; d\Omega + \int_{\Gamma_t} \delta\boldsymbol{u}^T \boldsymbol{t}^*\; d\Gamma
\end{aligned} \tag{13}$$

where α and β are nondimensional stabilization parameters ($\alpha \geq 0$ and $\beta \geq 0$), h is the length parameter of the mesh, and $[[\cdot]]$ is the jump operator. The "pressure jump" in $p_n = p_i n_i$ at $\boldsymbol{x}$ is defined as $[[p_n]] = p_i^+ n_i^+ + p_i^- n_i^-$ where n_i^+ and n_i^- are the unit normals to the interior side i and the sign + or - is (arbitrarily) designated to be "+" in one side of $\tilde{\Gamma}$ and to be "−" in the other. The domain $\tilde{\Omega}$ denotes element interiors, and $\tilde{\Gamma}$ consists of the element interfaces. The above weak formulation involves the addition of "least-squares" forms of the following residuals: the equilibrium equation residual and the pressure continuity residual on element interfaces. These terms render the formulation to be coercive, in contrast to the classic

Galerkin formulation, and enable the Babuška-Brezzi condition to be avoided. Thus this formulation can provide stable pressure solutions for seemingly arbitrary combinations of displacement and pressure interpolations. In the above formulation, however, a careful choice of the parameters is required to prevent a loss of accuracy in the solution. Note that, in low order element such as Q1P0, div $\boldsymbol{\sigma}$ almost vanishes and only the pressure continuity residual is left.

3. QBI element formulation using γ-projection operator

3.1. Hu-Washizu variational principle

For isotropic incompressible materials, the stress $\boldsymbol{\sigma}$ can be split into two parts as

$$\sigma_{ij} = \tau_{ij} - p\,\delta_{ij} \tag{14}$$

Here, τ_{ij} denotes the deviatoric stress given by $\tau_{ij}=2\mu\varepsilon_{ij}\equiv 2\mu e_{ij}$ where e_{ij} is the deviatoric strain, p is the hydrostatic pressure defined as $p = -\frac{1}{n_{sd}}\sigma_{ii}$, and δ_{ij} is the Kronecker deita (δ_{ij}=1 if i=j, and δ_{ij}=0 otherwise).

The three-field Hu-Washizu variational principle for this material is

$$\prod^{HW} \int_{\Omega}[\frac{1}{2}\varepsilon_{ij}\,2\mu\varepsilon_{ij} - \tau_{ij}(\varepsilon_{ij} - u_{(i,j)}) - pu_{i,i}]\,d\Omega - W^{ext} \tag{15}$$

The matrix form of Eq. (15) with a pressure continuity residual for stabilization of pressure is

$$\begin{aligned}\prod^{HW}(\boldsymbol{u},\boldsymbol{\varepsilon},\boldsymbol{\tau},p) = {} & \int_{\Omega}[\frac{1}{2}\boldsymbol{\varepsilon}^T\boldsymbol{D}^{dev}\boldsymbol{\varepsilon} - \boldsymbol{\tau}^T(\boldsymbol{\varepsilon}-\nabla_s\boldsymbol{u}) - p(\operatorname{div}\boldsymbol{u})]\,d\Omega \\ & - \frac{\bar{\beta}}{2}\int_{\tilde{\Gamma}}[[p]]^2\,d\Gamma - W^{ext}\end{aligned} \tag{16}$$

where $\bar{\beta}=\beta h/2\mu$. The above functional, when the pressure residual term is excluded, is the standard Hu-Washizu form for incompressible materials where p is the Lagrange multiplier on the isochoric constraint $u_{i,i}$=0. For nearly incompressible materials, a perturbed Lagrangian approach is taken (see Oden and Carey, 1983) where an additional term, $\frac{1}{2\lambda}p^2$, is added to the functional. Taking stationary condition then gives the following weak form:

$$\begin{aligned}&\int_{\Omega}[\delta\boldsymbol{\varepsilon}^T(\boldsymbol{D}^{dev}\boldsymbol{\varepsilon}-\boldsymbol{\tau}) - \delta\boldsymbol{\tau}^T(\boldsymbol{\varepsilon}-\nabla_s\boldsymbol{u}) - \delta p(\operatorname{div}\boldsymbol{u}) + \delta(\nabla_s\boldsymbol{u})^T\boldsymbol{\tau} - \delta(\operatorname{div}\boldsymbol{u})^T p)]\,d\Omega \\ &\quad - \bar{\beta}\int_{\tilde{\Gamma}}[[\delta p]][[p]]\,d\Gamma - \delta W^{ext} = 0\end{aligned} \tag{17}$$

3.2. Finite element formulation for QBI-HF

We develop here the equations for the QBI element (Belytschko and Bachrach 1986) stabilized by the Hughes-Franca techniques, and it will be called QBI-HF. Using a projection operator suggested by Belytschko and Bachrach (1986), $\boldsymbol{u}$, $\boldsymbol{\varepsilon}$ and $\boldsymbol{\tau}$ fields can be decoupled

with constant and linear parts to overcome locking problems. The displacement field for a bilinear, isoparametric quadrilateral can be written

$$\boldsymbol{u} = (\boldsymbol{\Delta}^T + \boldsymbol{x}\boldsymbol{b}_x^T + \boldsymbol{y}\boldsymbol{b}_y^T + \hbar\,\boldsymbol{\gamma}^T)\boldsymbol{d} = \boldsymbol{N}\boldsymbol{d} \tag{18}$$

where

$$\boldsymbol{\Delta}^T = \frac{1}{4}[\boldsymbol{a}^T - (\boldsymbol{a}^T\boldsymbol{x})\boldsymbol{b}_x^T - (\boldsymbol{a}^T\boldsymbol{y})\boldsymbol{b}_y^T] \tag{19}$$

$$\boldsymbol{\gamma}^T = \frac{1}{4}[\boldsymbol{h}^T - (\boldsymbol{h}^T\boldsymbol{x})\boldsymbol{b}_x^T - (\boldsymbol{h}^T\boldsymbol{y})\boldsymbol{b}_y^T] \tag{20}$$

$$\boldsymbol{b}_x^T = \frac{1}{2A}[y_{24}, y_{31}, y_{42}, y_{13}],\ \boldsymbol{b}_y^T = \frac{1}{2A}[x_{42}, x_{13}, x_{24}, x_{31}] \tag{21}$$

$$\hbar = \xi\eta \tag{22}$$

Here, the translation vector $\boldsymbol{a}$ and the hourglass vector $\boldsymbol{h}$ are defined by

$$\boldsymbol{a}^T = [1, 1, 1, 1], \quad \boldsymbol{h}^T = [1, -1, 1, -1] \tag{23}$$

$\boldsymbol{x}$ and $\boldsymbol{y}$ denote element nodal coordinate vectors, x_{IJ} denotes x_I-x_J, A is element area, and ξ and η are the referential coordinates, $\xi\in[-1, +1]$ and $\eta\in[-1, +1]$.

The symmetric part of displacement gradient and divergence of displacement derived from Eq. (18) are

$$\nabla_s \boldsymbol{u} = \begin{Bmatrix} u_{x,x} \\ u_{y,y} \\ u_{x,y} + u_{y,x} \end{Bmatrix} = \begin{bmatrix} \boldsymbol{b}_x^T + \hbar_{,x}\boldsymbol{\gamma}^T & \boldsymbol{0} \\ \boldsymbol{0} & \boldsymbol{b}_y^T + \hbar_{,y}\boldsymbol{\gamma}^T \\ \boldsymbol{b}_y^T + \hbar_{,y}\boldsymbol{\gamma}^T & \boldsymbol{b}_x^T + \hbar_{,x}\boldsymbol{\gamma}^T \end{bmatrix} \begin{Bmatrix} \boldsymbol{d}_x \\ \boldsymbol{d}_y \end{Bmatrix} \equiv \boldsymbol{B}\,\boldsymbol{d} \tag{24}$$

$$\text{div}\,\boldsymbol{u} = u_{x,x} + u_{y,y} = [\boldsymbol{b}_x^T + \hbar_{,x}\boldsymbol{\gamma}^T \quad \boldsymbol{b}_y^T + \hbar_{,y}\boldsymbol{\gamma}^T] \begin{Bmatrix} \boldsymbol{d}_x \\ \boldsymbol{d}_y \end{Bmatrix} \equiv \boldsymbol{H}\,\boldsymbol{d} \tag{25}$$

The strain, deviatoric stress, and pressure fields for QBI element can be defined as

$$\boldsymbol{\varepsilon} = \begin{bmatrix} 1 & 0 & 0 & \hbar_{,x} & -\bar{\nu}\,\hbar_{,y} \\ 0 & 1 & 0 & -\bar{\nu}\hbar_{,x} & \hbar_{,y} \\ 0 & 0 & 1 & 0 & 0 \end{bmatrix} \begin{Bmatrix} \bar{\varepsilon}_x \\ \bar{\varepsilon}_y \\ 2\bar{\varepsilon}_{xy} \\ q_x \\ q_y \end{Bmatrix} \equiv \boldsymbol{E}\,\boldsymbol{e} \tag{26}$$

$$\boldsymbol{\tau} = \begin{bmatrix} 1 & 0 & 0 & \hbar_{,x} & 0 \\ 0 & 1 & 0 & 0 & \hbar_{,y} \\ 0 & 0 & 1 & 0 & 0 \end{bmatrix} \begin{Bmatrix} \bar{\tau}_x \\ \bar{\tau}_y \\ 2\bar{\tau}_{xy} \\ Q_x \\ Q_y \end{Bmatrix} \equiv \boldsymbol{S}\,\boldsymbol{s} \tag{27}$$

$$p = N^p \boldsymbol{p} \tag{28}$$

where $\bar{\nu}=\nu$ for plane stress and $\bar{\nu}=\nu/(1-\nu)$ for plane strain. Note that $\bar{\varepsilon}_x$, $\bar{\varepsilon}_y$, and $2\bar{\varepsilon}_{xy}$ are the constant portions of the strain fields; $\bar{\tau}_x$, $\bar{\tau}_y$, and $\bar{\tau}_{xy}$ are the constant portions of the deviatoric stress fields. The pressure interpolation function N^p is [1] for constant pressure field. For detailed definition and explanation, see Belytschko and Bachrach (1986).

Substituting Eqs. (24)-(28) into Eq. (17), the weak formulation becomes

$$\int_\Omega [\delta \boldsymbol{e}^T \boldsymbol{E}^T (\boldsymbol{D}^{dev} \boldsymbol{E}\boldsymbol{e} - \boldsymbol{S}\boldsymbol{s}) - \delta \boldsymbol{s}^T \boldsymbol{S}^T (\boldsymbol{E}\boldsymbol{e} - \boldsymbol{B}\boldsymbol{d}) - \delta \boldsymbol{p}^T N^p \boldsymbol{H}\, \boldsymbol{d} + \delta \boldsymbol{d}^T (\boldsymbol{B}^T \boldsymbol{S}\boldsymbol{s} - \boldsymbol{H}^T N^p \boldsymbol{p}) d\Omega - \delta \boldsymbol{p}^T \boldsymbol{R}\boldsymbol{p} = \delta \boldsymbol{d}^T \boldsymbol{f}^{ext} \tag{29}$$

where $\boldsymbol{f}^{ext}$ is the external force vector, and $\boldsymbol{R}$ is the pressure continuity residual matrix as

$$\boldsymbol{R} = \bar{\beta} \sum_{e=1}^{N_{el}} \int_{\Gamma^e} [[N^p]]^2 \, d\Gamma \tag{30}$$

Using similar notation as Stolarski and Belytschko (1983), let

$$\bar{\boldsymbol{D}}^{dev} = \int_\Omega \boldsymbol{E}^T \boldsymbol{D}^{dev} \boldsymbol{E}\, d\Omega \tag{31}$$

$$\bar{\boldsymbol{E}} = \int_\Omega \boldsymbol{S}^T \boldsymbol{E}\, d\Omega \tag{32}$$

$$\bar{\boldsymbol{B}} = \int_\Omega \boldsymbol{S}^T \boldsymbol{B}\, d\Omega \tag{33}$$

$$\bar{\boldsymbol{H}} = \int_\Omega N^p \boldsymbol{H}\, d\Omega \tag{34}$$

Substituting Eqs. (31)-(34) into (29) gives the following relations:

$$\bar{\boldsymbol{B}}^T \boldsymbol{s} - \bar{\boldsymbol{H}}^T \boldsymbol{p} = \boldsymbol{f}^{ext} \tag{35}$$

$$\bar{\boldsymbol{H}}\boldsymbol{d} + \boldsymbol{R}\boldsymbol{p} = 0 \tag{36}$$

$$\bar{\boldsymbol{D}}^{dev} \boldsymbol{e} - \bar{\boldsymbol{E}}^T \boldsymbol{s} = 0 \tag{37}$$

$$\bar{\boldsymbol{B}}\boldsymbol{d} - \bar{\boldsymbol{E}}\boldsymbol{e} = 0 \tag{38}$$

Eliminating $\boldsymbol{e}$ and $\boldsymbol{s}$ from Eqs. (35)-(38) gives the following matrix equation

$$\begin{bmatrix} \boldsymbol{K} & -\bar{\boldsymbol{H}}^T \\ -\bar{\boldsymbol{H}} & -\boldsymbol{R} \end{bmatrix} \begin{Bmatrix} \boldsymbol{d} \\ \boldsymbol{p} \end{Bmatrix} = \begin{Bmatrix} \boldsymbol{f}^{ext} \\ \boldsymbol{0} \end{Bmatrix} \tag{39}$$

where

$$\boldsymbol{K} = \bar{\boldsymbol{B}}^T \bar{\boldsymbol{E}}^{-T} \bar{\boldsymbol{D}}^{dev} \bar{\boldsymbol{E}}^{-1} \bar{\boldsymbol{B}} \tag{40}$$

4. Numerical examples

The accuracy and the stability of displacement and pressure solutions in QBI-HF will be

studied for various values of the stability parameter β. Note that when the parameter β is equal to zero, i.e., $\bar{\beta}$ =0, the weak form Eq. (17) becomes the conventional formulations which fail the Babuška-Brezzi stability condition.

For the convergence study, the displacement norm (L_2 norm) can be calculated as

$$\text{displacement norm} = [\int_{\Omega} (\boldsymbol{u} - \boldsymbol{u}^h)^T (\boldsymbol{u} - \boldsymbol{u}^h) d\Omega]^{1/2} \tag{41}$$

and the energy norm (H_1 norm) for compressible or nearly incompressible materials can be calculated by

$$\text{energy norm} = [\frac{1}{2} \int_{\Omega} (\boldsymbol{\varepsilon} - \boldsymbol{\varepsilon}^h)^T \boldsymbol{D} (\boldsymbol{\varepsilon} - \boldsymbol{\varepsilon}^h) d\Omega]^{1/2} \tag{42}$$

For incompressible plane strain, Eq. (42) can not be used because the stress-stain matrix $\boldsymbol{D}$ is not defined when ν is 0.5. the energy norm can be decomposed into the deviatoric energy norm and the pressure norm as

$$\text{deviatoric energy norm} = [\frac{1}{2} \int_{\Omega} (\boldsymbol{\varepsilon} - \boldsymbol{\varepsilon}^h)^T \boldsymbol{D}^{dev} (\boldsymbol{\varepsilon} - \boldsymbol{\varepsilon}^h) d\Omega]^{1/2} \tag{43}$$

$$\text{pressure norm} = [\int_{\Omega} (\boldsymbol{p} - \boldsymbol{p}^h)^T (\boldsymbol{p} - \boldsymbol{p}^h) d\Omega]^{1/2} \tag{44}$$

Both errors in the deviatoric strain energy and pressure are considered.

4.1. Timoshenko beam problem

The test problem is a linear, elastic cantilever with a load P at its end as shown in Fig. 1 (Timoshenko and Goodier 1970). Assume there is no body force, and that the boundary conditions are given as follows:

(displacement)

$$u_x(0,\ 0) = u_y(0,\ 0) = 0,\ u_x(0,\ \pm c) = 0 \tag{45}$$

(traction)

$$t_x(x, \pm c) = t_y(x, \pm c) = 0, \quad x \in (0, L) \tag{46}$$

$$t_x(L, y) = 0, \tag{47a}$$

$$t_y(L, y) = \frac{P}{2I}(c^2 - y^2), \quad x = L, y \in (-c, c) \tag{47b}$$

$$t_x(0, y) = \frac{PLy}{I} \tag{48a}$$

$$t_y(0, y) = -\frac{P}{2I}(c^2 - y^2) \quad x = 0, y \in (-c, 0) \cup (0, c) \tag{48b}$$

where the moment of inertia, $I=d^3/12$.

The traction boundary conditions are those encountered in simple bending theory for a cantilever beam with root section at x=0, with parabolically varying end shear and linearly-varying bending stress at the root. The displacement boundary conditions allow the root section to warp.

The exact solution of this problem is

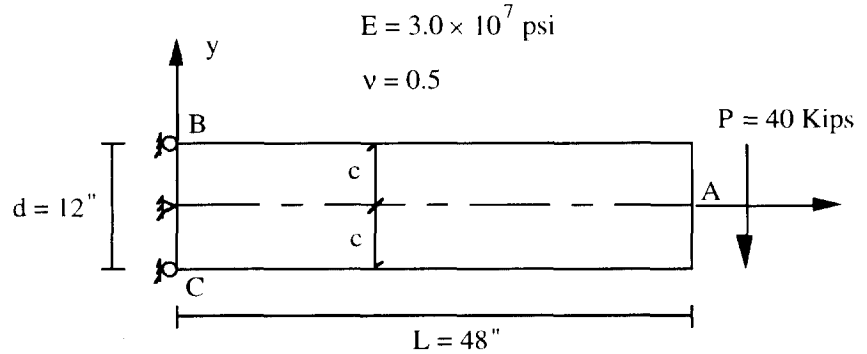

Fig. 1 Linear elastic Timoshenko beam bending problem

$$u_x(x,y)=\frac{-Py}{6\bar{E}I}[(6L-3x)x+(2+\bar{\nu})(y^2-\frac{1}{4}d^2)] \tag{49}$$

$$u_y(x,y)=\frac{P}{6\bar{E}I}[3\bar{\nu}y^2(L-x)+\frac{1}{4}(4+5\bar{\nu})d^2x+(3L-x)x^2] \tag{50}$$

$$\sigma_x=-\frac{Py}{I}(L-x) \tag{51}$$

$$\sigma_y=0 \tag{52}$$

$$\sigma_{xy}=\frac{P}{2I}(\frac{1}{4}d^2-y^2) \tag{53}$$

and the pressure solution for incompressible case is

$$p=\frac{Py}{2I}(L-x). \tag{54}$$

Here, $\bar{E}=E$ and $\bar{\nu}=\nu$ for plane stress, and $\bar{E}=E/(1-\nu^2)$ and $\bar{\nu}=\nu/(1-\nu)$ for plane strain.

In the convergence study of this beam problem, incompressible material or nearly incompressible materials are considered because both volumetric locking and pressure oscillations (or pressure modes) occur in this case. A state of plane strain is assumed.

For various values of β (from 0.0001 to 10.0), the y-deflections at point A by QBI-HF and Q1P0-HF (standard bilinear displacement-constant pressure four-node quadrilateral element with the stabilization term) are given in Tables 1 and 2, respectively. The convergence rates

Table 1 Deflections of QBI-HF in Timoshenko beam problem with the traction boundary condition

No. of element	Deflections at point A (u_{FEM}/u_{exact}) according to the variation of β								
	0.0001	0.001	0.005	0.01	0.05	0.1	0.5	1.0	10.0
8	0.983	0.985	0.997	1.011	1.100	1.175	1.382	1.445	1.521
32	0.995	0.996	0.997	0.999	1.013	1.029	1.131	1.224	1.636
128	0.998	0.999	0.999	1.000	1.002	1.005	1.020	1.033	1.191
512	1.000	1.000	1.000	1.000	1.000	1.001	1.004	1.007	1.031

Table 2 Deflections of Q1P0-HF in Timoshenko beam problem with the traction boundary condition

No. of element	Deflections at point A (u_{FEM}/u_{exact}) according to the variation of β								
	0.0001	0.001	0.005	0.01	0.05	0.1	0.5	1.0	10.0
8	0.885	0.887	0.896	0.906	0.974	1.031	1.182	1.226	1.279
32	0.964	0.964	0.966	0.968	0.981	0.995	1.089	1.176	1.550
128	0.990	0.990	0.990	0.990	0.993	0.995	1.010	1.022	1.177
512	0.997	0.997	0.997	0.997	0.998	0.998	1.001	1.004	1.028

of displacement norms are shown in Figs. 2 and 3. The y-deflections in Tables 1 and 2 show that the stiffness matrix becomes more flexible as the stability parameter β increases. In the accuracy of displacement solutions, as shown in Figs. 2 and 3, the QBI-HF is superior to the Q1P0-HF. The rates of convergence of displacement norms are approximately $O(h^2)$. For large β values (β>0.1), the rate of convergence is slightly greater than 2 and the accuracy of displacement solutions decreases significantly. The convergence rates of deviatoric energy norms and pressure norms by QBI-HF are shown in Figs. 4 and 5, respectively. The rate of convergence is approximately $O(h^1)$. It is also shown that for large β, the errors in energy norms and pressure norms increase.

In Figs. 6 and 7, the errors in displacement norm and the energy norm of the QBI-HF are compared with those of other several elements; QM6 element by Taylor *et al.* (1976), Simo and Rifai's element (1990), and ASQBI element by Belytschko and Bindeman (1991). Poisson's ratio ν=0.4999 in QM6, Simo and Rifai's element, and ASQBI; whereas ν=0.5 in QBI-HF and Q1P0-HF. The QBI-HF element shows the best accuracy in the displacement.

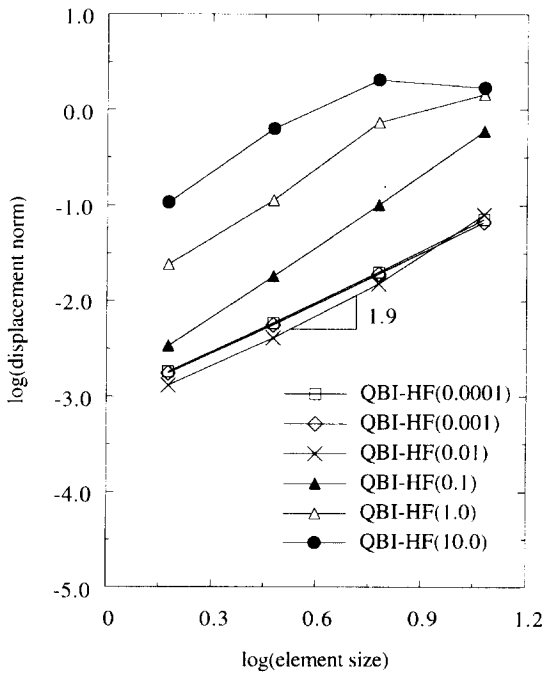

Fig. 2 Convergence rates of displacement norms in QBI-HF; quantity enclosed in parenthesis is the parameter β

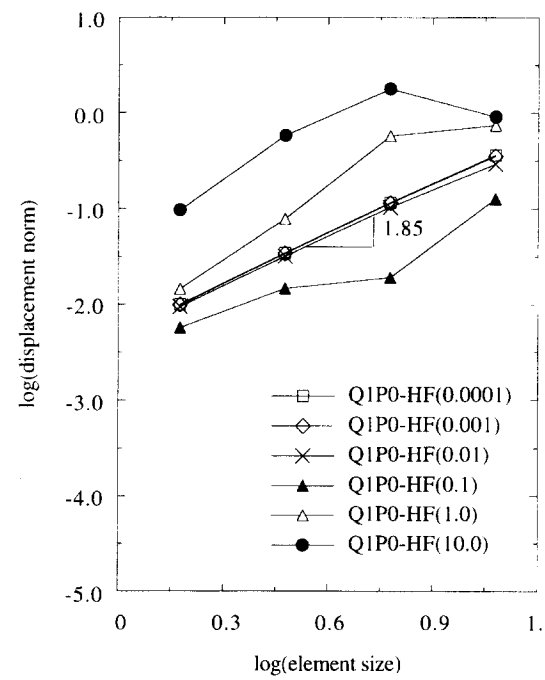

Fig. 3 Convergence rates of displacement norms in Q1P0-HF

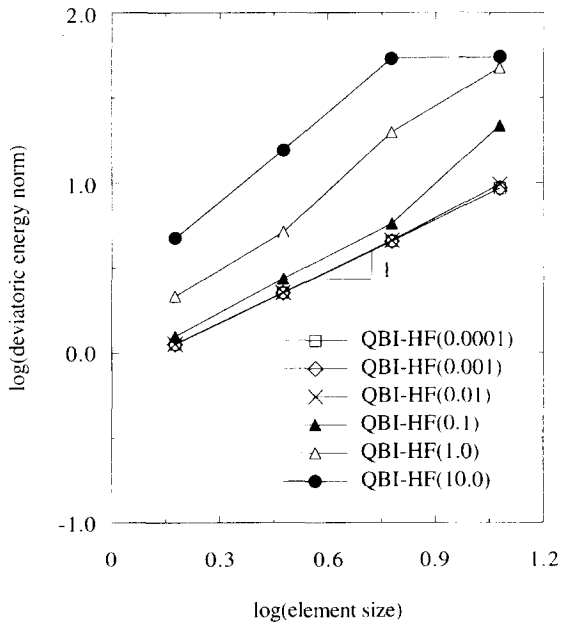

Fig. 4 Convergence rates of deviatoric energy norms in QBI-HF

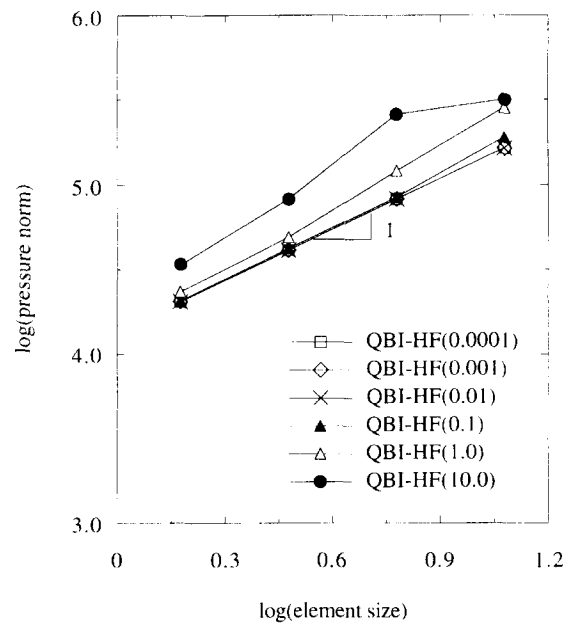

Fig. 5 Convergence rates of pressure norms in QBI-HF

The pressure solutions of QBI-HF for the prescribed displacement boundary conditions are shown in Fig. 8, where the pressure distributions at x=22.5 for various values of β are compared with exact pressures. The pressure solutions of Simo-Rifai are also presented. The pressure solutions show an oscillation for $\beta \leq 0.0001$, and the solutions become erratic for $\beta >$ 0.1. In other words, the pressure solutions are unstable for small β values, and they seem to

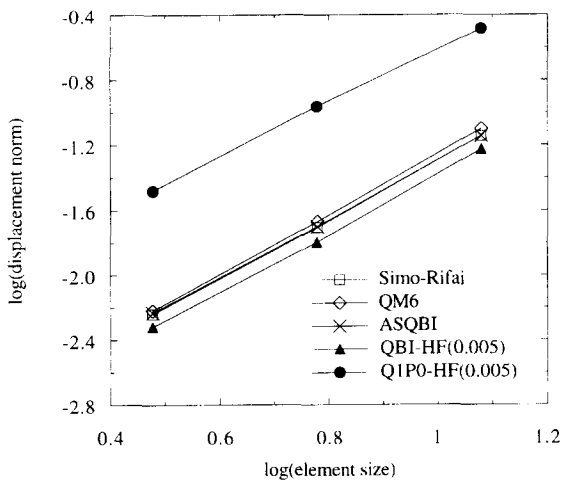

Fig. 6 Convergence rates of displacement norms in several elements (ν=0.4999 in QM6, Simo-Rifai, and ASQBI; ν=0.5 and β=0.005 in QBI-HF and Q1P0-HF)

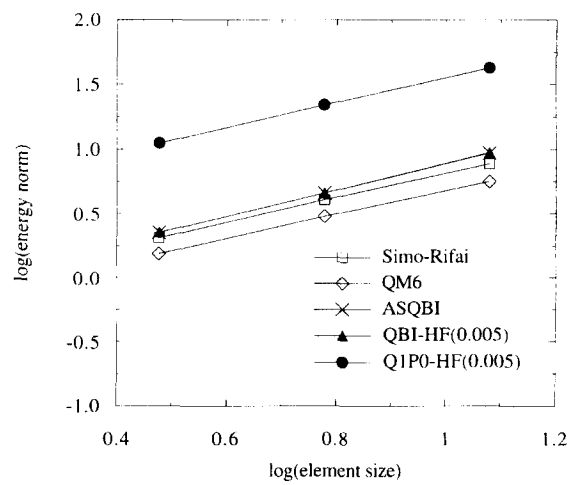

Fig. 7 Convergence rates of energy norms in several elements (ν=0.4999 in QM6, Simo-Rifai, and ASQBI; ν=0.5 and β=0.005 in QBI-HF and Q1P0-HF)

be stable but not accurate for large β values in which the accuracy of displacement solutions is also poor. For the range of $0.001 \leq \beta \leq 0.1$, the pressure solutions are stable and accurate and the displacement solutions are accurate. These phenomena can be observed more clearly in the next example.

4.2. Pressure modes in Timoshenko beam problem

The well known benchmark problem for observing *pressure oscillations* or *pressure modes* is the cavity flow problem. This problem has been cited frequently; however, no closed form solution is available for velocities (displacements) or pressures. Consequently, considerable difficulties arise in evaluating techniques for the elimination of *pressure oscillations* or *pressure modes* by means of this problem. Here, a study on the stabilization of pressure solutions is performed by capturing the *pressure modes* in the Timoshenko beam bending problem.

In order to capture the pressure modes in the beam, the boundary condition at x=0 in Eq. (50) is modified so that u_y=0 at points B and C of Fig. 1. The introduction of this perturbation makes the pressure solutions of the beam problem highly oscillatory for unstable elements. In this case, exact solutions given in Eqs. (49)-(54) are not valid any more, however the elimination of pressure oscillations or pressure modes can be studied successfully.

The pressure distributions at x=22.5 for various values of β under the additional displacement perturbation condition are shown in Fig. 9. The pressure distributions of other elements exhibit the *pressure modes* under this constraint condition. The *pressure modes* observed in Simo-Rifai element are shown in Fig. 10. In Fig. 9, the pressure distributions for small β values ($\beta \leq 0.0001$) are not shown because the pressures oscillate severely. As β

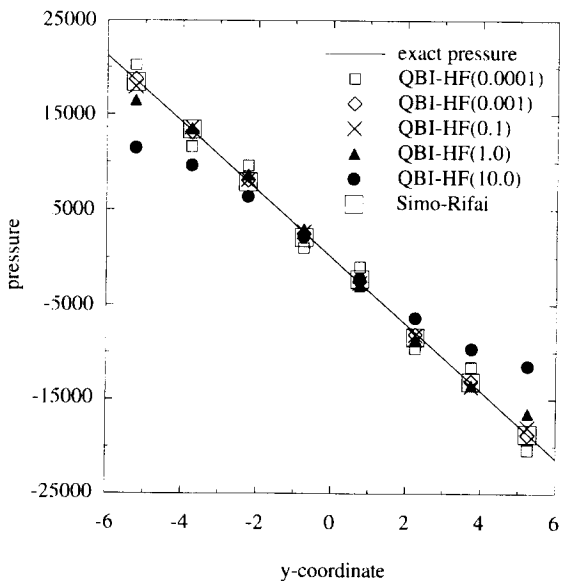

Fig. 8 Pressure distributions at x=22.5 in Timoshenko beam problem with the prescribed displacement boundary condition (QBI-HF)

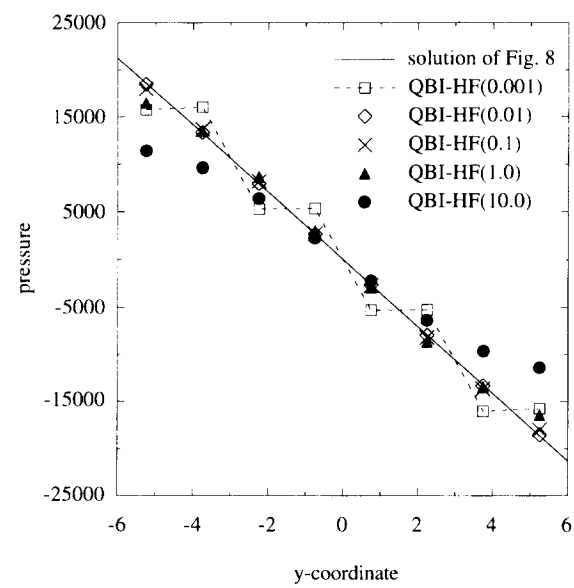

Fig. 9 Pressure distributions at x=22.5 in Timoshenko beam problem with the prescribed displacement boundary condition and the perturbed displacement boundary condition (QBI-HF)

increases, the oscillations diminish and the pressure solutions become stable and accurate. For large β values (β>0.1) the pressure solutions become erratic.

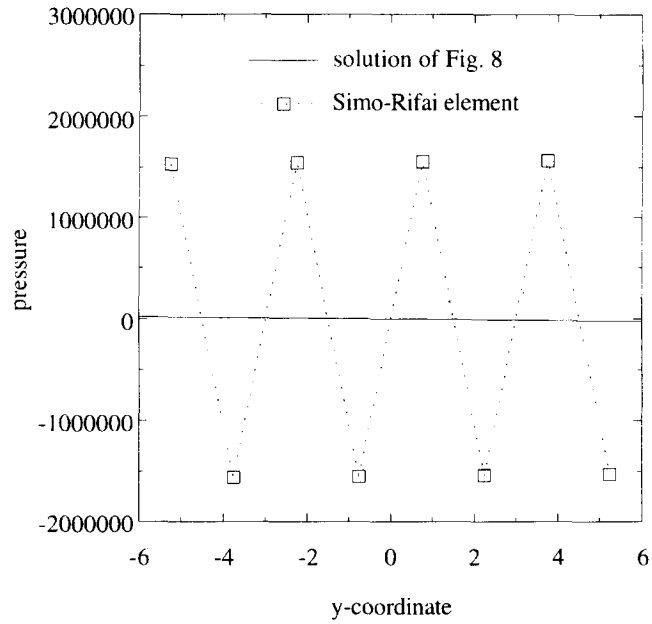

Fig. 10 The *pressure modes* observed at x=22.5 in Timoshenko beam problem with the prescribed displacement boundary condition and the perturbed boundary condition (Simo-Rifai element)

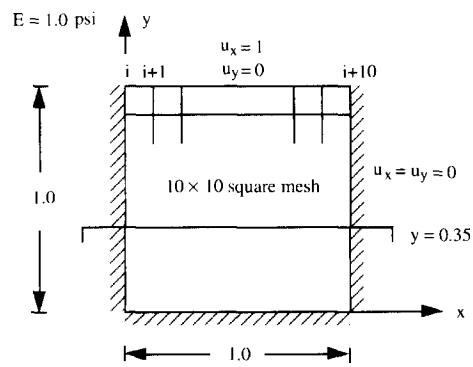

Prescribed displacement boundary conditions

Case A	Case B
$u_x^i = u_x^{i+1} = \cdots = u_x^{i+10} = 1.0$	$u_x^{i+1} = \cdots = u_x^{i+9} = 1.0,\ u_x^i = u_x^{i+10} = 0$
$u_x = u_y = 0$ elsewhere on Γ	$u_x = u_y = 0$ elsewhere on Γ

Prescribed displacement boundary conditions

Case A	Case B
$u_x^i = u_x^{i+1} = \cdots = u_x^{i+10} = 1.0$	$u_x^{i+1} = \cdots = u_x^{i+9} = 1.0,\ u_x^i = u_x^{i+10} = 1.0$
$u_x = u_y = 0$ elsewhere on Γ	$u_x = u_y = 0$ elsewhere on Γ

Fig. 11 Driven cavity flow model and two different boundary conditions

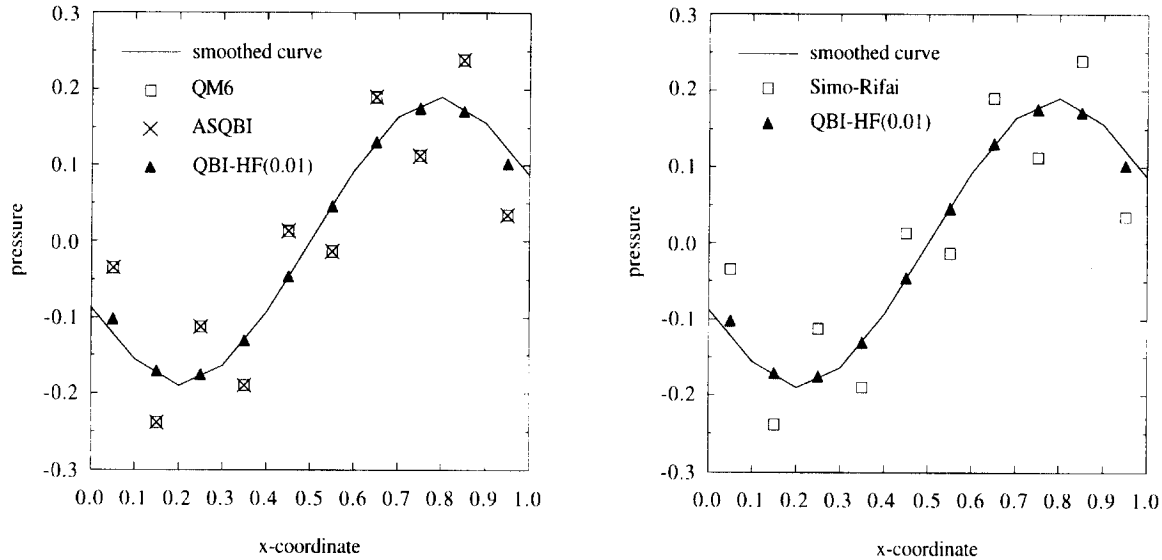

Fig. 12 Pressure distributions at y=0.35 in the driven cavity flow problem with the boundary condition Case A (ν=0.4999 in QM6, Simo-Rifai, and ASQBI; ν=0.5 and β=0.01 in QBI-HF)

4.3. Driven cavity flow problem

The last example is the well known driven cavity flow problem. The geometry of the model and the applied boundary conditions are shown in Fig. 11. Two different boundary conditions have been used; one of which, Case A (often called 'leaky lid' boundary condition),

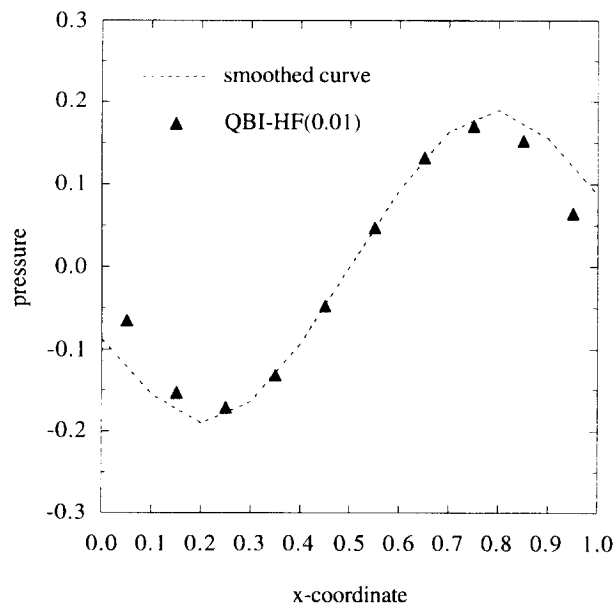

Fig. 13 Pressure distributions at y=0.35 in the driven cavity flow problem with the boundary condition Case B (ν=0.5 and β=0.01 in QBI-HF)
*Other elements show severe *pressure modes.*

causes *pressure oscillations* and the other, Case B (often called 'ramp over one element' boundary condition), causes *pressure modes* in conventional finite element analyses. In this example, the stability parameter β=0.01 was used.

The distribution of pressures at y=0.35 for QBI-HF and other several elements is shown in Fig. 12 where the boundary condition Case A has been used. The smoothed curve obtained by post processing, see (Lee *et al.* 1979), is considered as the benchmark solution. The pressures of QM6, Simo and Rifai's element and ASQBI are oscillatory whereas those of QBI-HF are stable and accurate. Although not shown, Pian and Sumihara (1984) and QBI (Belytschko and Bachrach, 1986) exhibit similar instabilities. The distribution of pressures in the boundary condition Case B is shown in Fig. 13. This boundary condition makes the pressure solutions of conventional methods more unstable. The pressures of QM6, Simo and Rifai's element, and ASQBI show severe *checkerboarding* and could not be shown in Fig. 13 without obscuring the benchmark solution. The pressures of QBI-HF are also stable in this case.

5. Summary and conclusions

The stabilization procedure of Hughes and Franca has been studied in the context of a four-node quadrilateral element with a strain field designed to avoid volumetric locking. It has been shown that this stabilization avoids the pressure oscillations which plague these elements for incompressible materials. Numerical examples showed that the performance of the proposed element, QBI-HF, is superior to that of other conventional elements and Q1P0-HF. Even in special displacement boundary condition problems which cause severe pressure mode in incompressible case, QBI-HF showed a good and stable performance. However, the results are still sensitive to the stabilization parameter as summarized below:

1) For $0<\beta\leq 0.001$: *Pressure oscillations* or *pressure modes* can not be eliminated successfully.
2) For $0.001<\beta\leq 0.1$: *Pressure oscillations or pressure modes* are eliminated successfully. Pressure solutions are stable and accurate. Displacement solutions are still accurate (there is no significant loss of accuracy in the displacement solutions).
3) For $0.5\leq 10.0$: *Pressure oscillations* or *pressure modes* are eliminated but the pressure solutions become poor as β increases. The displacement solution loses its accuracy as β increases.

As a byproduct of this investigation, we have identified an excellent problem for checking the stability of plane elements: the Timoshenko beam problem with a perturbed boundary condition. It has shown with this test that many well known mixed elements are also unstable as the material becomes incompressible. In particular, the Pian-Sumihara and Simo-Rifai elements both suffer from pressure oscillations in this problems. Similarly, the QBI element of Belytschko and Bachrach suffers pressure oscillations unless the Hughes-Franca stabilization is added.

Acknowledgements

The guidance and helpful discussion of professor Belytschko at Northwestern University are gratefully acknowledged.

References

Babuška, I. (1971), "Error bounds for finite element method", *Numer. Math.*, **16**, 322-333.

Belytschko, T. and Bachrach, W.E. (1986), "Efficient implementation of quadrilateral with high coarse-mesh accuracy", *Comput. Meths. Appl. Mech. Engrg.*, **54**, 279-301.

Belytschko, T. and Bindeman, L.P. (1991), "Assumed strain stabilization of the 4-node quadrilateral with 1-point quadrature for nonlinear problems", *Comput. Meths. Appl. Mech. Engrg.*, **88**, 311-340.

Brezzi, F. (1974), "On the existence, uniqueness and approximation of saddle-point problems arising from Lagrange multipliers", *RAIRO Ser. Rouge Anal. Numér.*, **R-2**, 129-151.

Doherty, W.P., Wilson, E.L. and Taylor, R.L. (1969), "Stress analysis of axisymmetric solids utilizing higher order quadrilateral finite elements", SESM Report No. 69-3, Department of Civil Engineering, University of California, Berkeley, CA.

Hughes, T.J.R. (1977), "Equivalence of finite elements for nearly incompressible elasticity", *J. Appl. Mech.*, **44**, 181-183.

Hughes, T.J.R. (1987), The Finite Element Method: Linear Static and Dynamic Finite Element Analysis, Prentice-Hall, Englewood cliff, NJ.

Hughes, T.J.R. and Franca, L.P. (1987), "A new finite element formulation for computational fluid dynamics: VII. The Stokes problem with various well-posed boundary conditions: Symmetric formulations that converge for all velocity/pressure spaces", *Comput. Meths. Appl. Mech. Engrg.*, **65**, 85-96.

Lee, R.L., Gresho, P.M. and Sani, R.L. (1979), "Smoothing techniques for certain primitive variable solutions of the Navier-Stokes equations", *Internat. J. Numer. Meths. Engrg.*, **14**, 1785-1804.

MacNeal, R.H. (1993), Finite Elements: Their Design and Performance, Marcel Dekker Inc., New York.

Malkus, D.S. and Hughes, T.J.R. (1978), "Mixed finite element methods-reduced and selective integration technique: a unification of concepts", *Comput. Meths. Appl. Mech. Engrg.*, **15**, 63-81.

Oden. J.T. and Carey, G. (1983), Finite Elements: Mathematical Aspects, Prentice-Hall, Inc., Englewood Cliffs, New Jersey.

Oden. J.T., Kikuchi, N. and Song, Y.J. (1982), "Penalty-finite element methods for the analysis of Stokesian Flows", *Comput. Meths. Appl. Mech. Engrg.*, **31**, 297-329.

Pian, T.H.H. and Sumihara, K. (1984), "Rational approach for assumed stress finite elements", *Internat. J. Numer. Meths. Engrg.*, **20**, 1685-1695.

Pitkäranta, J. and Saarinen, T. (1985), "A multigrid version of a simple finite element method for the Stokes problem", *Math. Comp.*, **45**, 1-14.

Pitkäranta, J. and Stenberg, R. (1984), "Error bounds for the approximation of the Stokes problem using bilinear/constant elements on irregular quadrilateral meshes", Report-MAT-A222, Helsinki University of Technology, Institute of Mathematics, Finland.

Sani, R.L., Gresho, P.M., Lee, R.L., Griffiths, D. F. and Engleman, M. (1981), "The cause and cure (?) of the spurious pressures generated by certain FEM solutions of the incompressible Navior-Stokes equations: Part I and Part II", *Internat. J. Numer. Meths. in Fluids*, **1**, 17-43 and 171-204.

Silvester, D.J. and Kechkar, N. (1990), "Stabilised bilinear-constant velocity-pressure finite elements for the conjugate gradient solution of the Stokes problem", *Comput. Meths. Appl. Mech. Engrg.*, **79**, 71-86.

Simo, J.C. and Rifai, M.S. (1990), "A class of mixed assumed strain methods and the method of incompressible modes", *Internat. J. Numer. Meths. Engrg.*, **29**, 1595-1638.

Stolarski, H. and Belytschko, T. (1983), "Shear and membrane locking in curved C^0 elements", *Comput. Meths. Appl. Mech. Engrg.*, **41**, 279-296.

Taylor, R.L., Beresford, P.J. and Wilson, E.L. (1976), "A non-conforming element for stress analysis", *Internat. J. Numer. Meths. Engrg.*, **10**, 1211-1219.

Taylor, C. and Hood, P. (1973), "A numerical solution of the Navior-Stokes equations using FEM techniques", *Computers and Fluids*, **1**, 73-100.

Timoshenko, S.P. and Goodier, J.N. (1970), Theory of Elasticity 3rd ed., McGraw-Hill book company, 41-46.

Xue, W-M., Karlovitz, L.A. and Atluri, S.N. (1985), "On the existence and stability conditions for mixed-hybrid finite element solutions based on Reissner? variational principle", *Intl. J. Solids Structures*, **21**, 97-116.